Mol Cell Biochem (2018) 442:81–96
https://doi.org/10.1007/s11010-017-3195-6

Mode of treatment governs curcumin response on doxorubicin-induced toxicity in cardiomyoblasts

Aditi Jain[1] · Vibha Rani[1]

Received: 10 July 2017 / Accepted: 9 September 2017 / Published online: 19 September 2017

Abstract Doxorubicin (Dox) is an effective anti-cancer drug with severe reported cardiotoxicity. Cardiovascular risks associated with present cancer therapeutics demand urgent attention. There has been a growing interest in naturally occurring compounds to improve the therapeutic index as well as prevent non-tumour tissues from sustaining chemotherapy-induced damages. In the present study, the effects of curcumin, a polyphenol isolated from *Curcuma longa* and well known for its anti-oxidative, anti-cancerous and anti-inflammatory properties, was studied in relation to the Dox-induced cardiotoxicity. As literature suggests conflicting role of curcumin in Dox-induced cardiotoxicity, concentration- and time-dependent studies were conducted to study the different curcumin effects. H9C2 cardiomyoblasts were used in the study and cell viability assays were done to study Dox-induced cellular death. Drug uptake assay for Dox was performed followed by cellular growth inhibition analysis by FACS Calibur. Morphological alterations, intracellular ROS levels and mitochondrial integrity were observed by fluorescent-based microscopic studies. Catalases and superoxide dismutase-inbuilt anti-oxidant enzyme activities were studied, and it was observed that Dox-dependent cardiotoxicity occurs through ROS overproduction by exaggerating the inbuilt anti-oxidant mechanism. Expression analysis for cell death and ROS markers—BCl_2, Bax, SOD, catalase—was investigated by semi-quantitative RT-PCR, and the Dox-induced stress on cardiac cells was confirmed. Initiator and effector caspases activity analysis also confirmed these findings. Our study proposes that curcumin exerts time-dependent responses on Dox-induced cardiotoxicity, where parallel treatment potentiates and pre-treatment suppresses the Dox-induced toxicity in H9C2 cardiomyoblasts. In conclusion, pre-treatment of curcumin suppresses the Dox-induced cardiotoxicity and holds a great potential as future cardio-oncological therapeutics.

Keywords Anti-cancerous drug · Doxorubicin · Cardiotoxicity · Curcumin · Reactive oxygen species · Anti-oxidant

Introduction

World Health Organisation has put forward the fact that cardiovascular anomalies are a major cause of deaths worldwide and hence, cardiotoxicity has become a key concern for scientific community [1]. Cardiotoxicity takes place in response to any chemical molecule or due to the compromised working of cardiac cells and tissues. Drug-induced cardiotoxicity has withdrawn ample attention in past two decades and different classes of drugs including Rosiglitazone, Prenylamine, Rofecoxib, Levomethadyl acetate have been banned from the market as a result of associated severe cardiotoxicity [2–5]. However, there are still many cardiotoxic drugs that are being used by clinicians either because they outweigh the risk of cardiac deformities or due to the non-availability of other safer alternatives. Doxorubicin (Dox) is a well-known anti-cancerous drug with reported cardiotoxicity. Literature supports that time- and concentration-dependent Dox

✉ Vibha Rani
vibha.rani@jiit.ac.in; vibha.rani@gmail.com

Aditi Jain
aditijain506@gmail.com

[1] Department of Biotechnology, Jaypee Institute of Information Technology, A-10, Sector-62, Noida, Uttar Pradesh 201307, India

therapy induces toxicity and heart failure; however, the exact mechanism involved is poorly defined [6–9]. As a result, patients recover from cancer but decease because of cardiac complications during the course of time. Hence, there is a need to develop cardio-oncological preventive therapeutics to reduce the associated side effects of drugs [10].

Supplementing the drugs with compounds having protective effects can be a good approach to lessen the associated toxicity [11]. In this regard, we focus on natural compounds as they are comparatively less toxic with marginal or no side effects [12–14]. The concept is strengthened by recent literature where Dox-induced cardiotoxicity was suppressed by Schisandrin B—isolated from a fruit *Schisandra chinensis* and Sulforaphane—a natural isothiocyanate from cruciferous vegetables [15, 16]. Curcumin, a biphenyl compound present in nutritionally enriched *Curcuma longa* (Turmeric), known for its diverse potential including anti-oxidant, anti-inflammatory, anti-cancerous and anti-microbial properties was selected in the present study to analyse its effects against Dox-induced cardiotoxicity [17–22]. Oxidative abnormalities are believed to be a common link between cancer and cardiac toxicity. Curcumin being an established anti-oxidative compound therefore holds a great potential for cardio-oncological therapeutics. We have previously shown the cardioprotective potential of curcumin by inhibiting GATA-4-mediated cardiac fetal gene program and also regulating ECM remodelling [23, 24]. Our findings also showed that curcumin suppressed prolonged hypertrophy-induced cardiac cell death in vitro [25–27]. In the present study, we further extended our research to explore the cardioprotective potential of curcumin in anti-cancerous drug-induced cardiotoxicity, a serious concern for cancer patients worldwide. Though research has been conducted in this aspect by other groups as well, however, there has been contrasting results of curcumin effects. This makes the present study important to identify the exact responses showed by curcumin in Dox-induced cardiotoxicity. We hypothesised that mode of curcumin treatment could be an important parameter to deliver its effect on various cell systems [28, 29]. The role of curcumin as an anti-cancerous and cardioprotective agent is mechanistically opposite where it targets the cancer cells by activating apoptotic pathways and on the other hand suppresses apoptosis in terminally differentiated cardiomyocytes. There has been contrasting views in literature particularly for role of curcumin on Dox-induced cardiotoxicity that led us to explore actual curcumin-mediated effects in Dox-mediated cardiac complications in depth.

A study suggested that pre-treatment of curcumin one hour prior to Dox treatment potentiates cell death in H9C2 cells by excessive ROS generation [30]. However, other recent reports contradict that curcumin significantly improves Dox-induced alterations in pro- and anti-oxidant balance in neonatal rat cardiomyocytes [31–34]. Also, ethyl alcohol extract of *Curcuma longa* has been reported to prevent cardiac, hepatic and renal toxicities induced by Dox by scavenging free radicals [35]. To examine our hypothesis various comparative assays were conducted at different concentrations and time points.

Various parameters were investigated in the present study including cellular and nuclear alterations, intracellular ROS generation and anti-oxidant imbalance, cellular death pathways and their effect on the mitochondrial execution in H9C2 cardiomyoblasts—a significant experimental model to study the cardiac stress [36, 37]. Since the mechanisms and effects involved in curcumin-mediated responses against Dox-induced cardiotoxicity are not clearly known, this study sets a critical platform for the same.

Altogether, our experimental findings reflect that mode of curcumin treatment is a critical check-point for improving cardiac health in Dox-induced toxicity.

Materials and methods

All chemicals were purchased from Sigma-Aldrich, USA unless or otherwise mentioned.

Cell culture maintenance and treatment

Embryonic rat cardiac tissue-derived H9C2 cardiomyoblasts (NCCS, Pune, India) were cultured in DMEM supplemented with 10% FBS and antibiotics. Cells were grown at the density of 10^6 cells/cm^2 in a humidified incubator with 5% CO_2 at 37 °C. Cells were grown in culture dish 16–18 h before the treatment. The experimental groups were divided into six groups: (i) untreated H9C2 cells (Control), (ii) Dox-treated cells with stress induction of 24 h (Dox), (iii) cells pre-treated with curcumin for 24 h followed by Dox treatment (Pre), (iv) cells simultaneously treated with curcumin and Dox (Concomitant or Parallel), (v) cells treated with DMSO and (vi) cells treated with curcumin alone. Curcumin used in the study has $> 80\%$ curcumin content (Catalogue number: C7727, Sigma-Aldrich).

MTT cell viability assay

MTT assay was done to measure the cytotoxicity and to optimise the concentrations of Dox and curcumin at different time points. Increasing concentrations of Dox and curcumin were used where Dox ranging from 1 to 20 μM was studied for 24 and 48 h separately to calculate its IC_{50}

dose. Curcumin alone ranging from 5 to 30 μM was used to derive its safe concentration. IC_{50} dose of Dox was further studied in combination with different curcumin concentrations. Following the treatments, viable cells were stained with 5 mg/ml MTT for 3 h. The media was replaced with DMSO in each well to solubilise formazan and absorbance was measured at 570 nm using spectrophotometer (Bio-Rad Laboratories-USA) [38]. Percent cell viability was calculated using the formula (Absorbance of treated cells)/(Absorbance of untreated cells).

Assessment of cellular uptake and cytotoxicity of Dox by FACS

A concentration-dependent study was conducted for the cells treated with fluorescent Dox to analyse the cellular drug uptake in a concentration-dependent manner by flow cytometry. Concentrations ranging from 1 to 20 μM for 24 h were used and recorded using FACS Calibur by measuring the changes in the fluorescence with different concentrations through forward scatter (BD Bioscience). Cells were also counterstained with Annexin/PI to observe the concentration-dependent alterations in cell size.

Trypan blue dye exclusion assay

Cells from the six experimental groups were pelleted down and incubated with 0.4% trypan blue stain in 1:1 ratio and kept at room temperature for 5 min [39]. The cell suspension was loaded into the Countess® II Automated Cell Counter (Invitrogen) to record the total concentration of cells, number of dead and live cells. To quantify the cell viability from all experimental groups, stain was eluted from the cells and absorbance was measured at 595 nm by spectrophotometer.

Morphological analysis of H9C2 cells

Cells treated with Dox and curcumin were analysed for altered cell size and morphology under an inverted microscope (Olympus) at ×10 magnification. Cells were grown in 10% FBS to observe the overall growth inhibition in presence of Dox. The total concentration of cells in the individual experimental group was also evaluated by Countess® II Automated Cell Counter.

Giemsa staining

Cellular morphology was studied by giemsa staining. Cells were fixed with 100% methanol at −20 °C and incubated with 20% giemsa stain diluted in 0.5% glacial acetic acid for 15 min at 25 °C and observed under an inverted microscope at ×100 magnification for morphological alterations [40]. Cell size was also quantified by NIH ImageJ software as per the instructions provided.

Haematoxylin–Eosin staining

Cells from all the experimental groups were assessed for sub-cellular morphological alterations by Haematoxylin–Eosin staining. Cells were washed with 1X PBS and fixed as mentioned above. 0.5% alcoholic haematoxylin was added to the cells and incubated for 30 min at 25 °C. Cells were then counterstained with 5% eosin for 10 min. Images were captured at ×100 magnification [41]. Cell size was also quantified by NIH ImageJ software.

DAPI nuclear staining

Changes in nuclear morphology of the cells treated with curcumin and Dox were observed in the presence of DAPI fluorescent stain. 50 ng/ml DAPI was prepared in the staining solution (10 mM Tris–Cl, pH 7.4; 10 mM EDTA, pH 8 and 100 mM NaCl) and cells were incubated in dark for 15 min at room temperature [42]. Cells were then observed under fluorescent microscope (Olympus) using the DAPI filter at 100X magnification with excitation and emission wavelength at 372 and 456 nm, respectively.

NBT assay for superoxide generation

H9C2 cells following the respective treatments were incubated with 0.3% nitroblue tetrazolium chloride (NBT) solution for 1 h in a humified incubator with 5% CO_2 at 37 °C. Cells were counterstained with safranin and observed under microscope at ×100 for the formation of blue formazan crystals. Percentage of NBT positive cells was also measured by solubilising the crystals with 2 M KOH and DMSO [43]. Absorbance was taken at 630 nm and stimulation index for superoxides production was calculated as the absorbance ratio of the treated and control cells.

DCFH-DA assay for intracellular ROS

Intracellular ROS production in the presence of Dox and curcumin was studied by 2′, 7′-dichlorofluorescin diacetate (DCFH-DA). Cells were seeded as mentioned above and followed by appropriate inductions; 5 μM of DCFH-DA stain was added to the cells and incubated in the dark at room temperature for 30 min [44]. Cells were then observed under the FITC filter at ×100 magnification with excitation and emission wavelength at 490 and 520 nm, respectively. The net fluorescence of the eluted stained cells from the treated cells (both detached and adherent)

was also measured by spectrofluorometer at the excitation of 490 nm and an emission wavelength of 520 nm.

Total cell protein extraction

Cells from all the experimental groups were pelleted down and washed with cold 1X PBS and incubated on ice for 1 h in 20 mM HEPES, 20% glycerol, 500 mM NaCl, 0.2 mM EDTA, 0.1% TRITON-X and protease inhibitor cocktail for cellular lysis. Cells were incubated on ice for 1 h with intermittent taping and centrifuged at 13,000 rpm for 15 min at 4 °C. The supernatant was carefully aliquoted in pre-chilled vials and stored at −80 °C. The total cell protein isolated was quantified using Bradford assay.

Catalase assay

30 µg/ml of protein extract was added to the 100 mM potassium phosphate buffer (pH 7.0) and the reaction was initiated by adding 20 mM H_2O_2. Continuous decrease of absorbance was recorded for 2 min and the enzyme activity was measured as U/mg of protein [45]. Purified Catalase enzyme was used to plot a standard.

Superoxide dismutase assay

Superoxide dismutase (SOD) activity was determined by the method of Beauchamp and Fridovich [46]. The reaction mixture with 100 mM potassium phosphate buffer-pH 7.8, 100 mM EDTA pH 8.0, 65 mM L-methionine, 750 mM NBT and 2 mM riboflavin was added to 50 µg/ml of total cell protein from each experimental group. The samples were kept under a direct light source for 30 min and tubes were kept in dark to terminate the reaction and absorbance was recorded at 560 nm. The activity was expressed as U/mg of cellular protein.

Measurement of mitochondrial membrane potential by Rhodamine 123 staining

To study the alterations in mitochondrial membrane potential, cells from the defined groups were incubated with Rhodamine 123 (10 µg/ml) in DMEM for 30 min in 5% CO_2 incubator at 37 °C. Coverslips were then washed with DMEM thrice and mounted on microscope slides [47]. Stained cells were examined under FITC filter at ×100 magnification with excitation and emission wavelength at 490 and 520 nm, respectively.

Caspase colorimetric protease assay

The activities of caspase-2, -3 and -9 were determined by using Caspase colorimetric protease assay sampler kit (Invitrogen) as per the manufacturer's instructions. Briefly, cells were lysed with the provided lysis buffer for 30 min on ice. The cellular lysate was centrifuged at 13,000 rpm for 10 min. The protein was quantified and 100 µg of protein was incubated with 4 mM of specific substrates VDVAD-*p*NA, DEVD-*p*NA and LEHD-*p*NA for caspase-2,-3 and -9, respectively, at 37 °C in dark for two hours, and absorbance was recorded at 405 nm in an ELISA reader.

Cell cycle arrest by sub-G1 cell growth analysis

Cell pellet was fixed in 70% ethanol and kept overnight at −20 °C. The cell suspension was centrifuged at 5000 rpm for 5 min and the pellet was washed thrice with 1X PBS and air dried to remove the traces of ethanol. 200 µl of PI cocktail (0.25% TRITON-X, 10 mg/ml RNase and 1 µg/ml Propidium iodide dye in 1X PBS) was added to each pellet and incubated at 37 °C in water bath for 1 h. Samples were then directly analysed by flow cytometry in PI/RNase A solution for 10,000 events [48].

TUNEL assay

DNA fragmentation of cells was detected by terminal deoxyribonucleotide transferase dUTP nick end labelling (TUNEL) using APO Brdu-TUNEL Labelling apoptosis detection kit (Invitrogen). 2×10^6 cells were suspended in 0.5 ml of 1X PBS and fixed with 1% paraformaldehyde on ice for 15 min. 70% ice cold ethanol was added and kept for 30 min at 20 °C. The cell pellets were re-suspended in 50 µl of DNA labelling solution and again incubated for 60 min. Cells were then spin down at 3000 rpm for 5 min and the pellet was incubated in the antibody staining solution and observed under fluorescence microscope using FITC filter to count the TUNEL positive cells. The percent apoptotic cells were calculated and represented as bar graph.

RT-PCR

Total RNA was extracted using TRIzol reagent from different groups. Total RNA was reverse transcribed using cDNA synthesis kit (Thermo Scientific). The product was PCR amplified under semi-quantitative conditions using gene-specific primers and β-actin as a loading control. Cyclic parameters were 95 °C for 5 min, 56 °C for 1 min and 72 °C for 30 s. After cycling, the reaction mixtures were upheld at 72 °C for additional 10 min. The sequences of the primers used are listed in Table 1.

Table 1 Primer sequences

Primer	Sequence
Bcl_2	(F) 5′-GTGGGATACTGGAGATGAAG-3′
	(R) 5′-GTAGCGACGAGAGAAGTCAT-3′
Bax	(F) 5′-CTTTTTGCTACAGGGTTTCA-3′
	(R) 5′-TGTATCCACATCAGCAATCA-3′
SOD	(F) 5′-GACCTGGAGATCTGGATG-3′
	(R) 5′-GTGGTTGGAGGTGTTCTG-3′
Catalase	(F) 5′-TACTACCCCAACAGCTT-3′
	(R) 5′-GCTAAGCCCTAATCTTTAA-3′
β-Actin	(F) 5′-CATCGTACTCCTGCTTGCTG-3′
	(R) 5′-CCTCTATGCCAACACAGTGC-3′

Statistical analysis

All the experiments were carried out in triplicates and repeated three times. All data were expressed as Mean + SEM and significance was evaluated by student's *T* test as well as two-way ANOVA. P value was calculated on comparing the data where $p < 0.05$.

Ethics statement

All animal cell culture work was performed in accordance with local ethical guidelines. The work was conducted on embryonic rat cardiac tissue-derived H9C2 cardiomyoblasts having biosafety level 1. Recently it has been shown that H9C2 cells display almost identical stress responses as compared to the primary cardiomyoblasts and thus can be used as a model for in vitro studies and no prior ethical approval is required for working with H9c2 cardiomyoblasts.

Results

Dox exerts concentration-dependent cell toxicity on H9C2 cardiomyoblasts

Cell viability assays were done to study the cellular death in the presence of Dox and to derive the cytotoxic IC_{50} concentration. Cardiac cells were treated with increasing concentrations of Dox followed by concentration and time-dependent MTT assay. It was observed that when cells were treated with 15 μM Dox for 24 h, cell viability was significantly declined by 50%. Cell viability for 48 h was also calculated and the concentration of 9 μM exerted 50% viability (Fig. 1a). Concentration-dependent cellular uptake of Dox was also studied by FACS where increase in Dox uptake as well as altered cell morphology was observed in a concentration-dependent manner (Fig. 1b). Trypan blue staining further validated the cellular death with increase in Dox concentrations where up to 40% cell death was observed at the concentration of 15 μM (Fig. 1c). Based on the results obtained, concentration of 15 μM Dox was selected as IC_{50} dose and used to induce stress for 24 h in all the experiments.

Mode of curcumin treatment exerts opposite effects on Dox-induced toxicity in vitro

To investigate the concentration of curcumin having protective effects on Dox toxicity, time-dependent cell viability assays for the combinations of Dox and curcumin were conducted. MTT assay for curcumin was performed with control cells to identify a concentration with minimum cytotoxicity. No significant cell death up to the concentration of 30 μM was observed where 20 μM curcumin showed 90% cell viability (Fig. 2a). Different time points of curcumin treatment, that is, pre and parallel treatments with the selected concentrations of curcumin were done using optimised Dox IC_{50} concentration for analysing the cell viability. We observed that pre-treatment of 20 μM curcumin resulted in increased cell viability up to 30% whereas parallel treatment of curcumin decreased the cell viability up to 15% in Dox-treated cells (Fig. 2b). As the concentration of 20 μM curcumin showed negligible cytotoxic effects when treated alone and decreased Dox effects up to 30% in pre-treatment, this concentration was selected for both pre and parallel treatments. Cell proliferation analysis by Trypan blue further confirmed the increase in cell viability by 25% in the curcumin pre-treated cells, and decreased cell viability by 15% in the parallel treated group with curcumin thereby confirmed time-dependent survival/detrimental effect of curcumin on Dox-induced toxicity (Fig. 2c).

Pre-treatment of curcumin prevents Dox-induced morphological alterations whereas parallel treatment exaggerates Dox-mediated toxic effects

Dox-mediated decrease in percentage cell viability was further validated by morphological analysis. Rounding off of H9C2 cells was observed in response to Dox treatment, while innate spindle-shaped cells were observed in control as well as pre-treated group. Increase in cell death and altered cellular morphology as well as reduced cell size was witnessed quantitatively in Dox-treated cardiac myoblasts that was further increased with parallel curcumin treatment. Reduced cellular death in curcumin pre-treatment thereby suggests its preventive potential. Overall cell growth was also observed upon various exposures in addition to the altered morphology. Significant growth

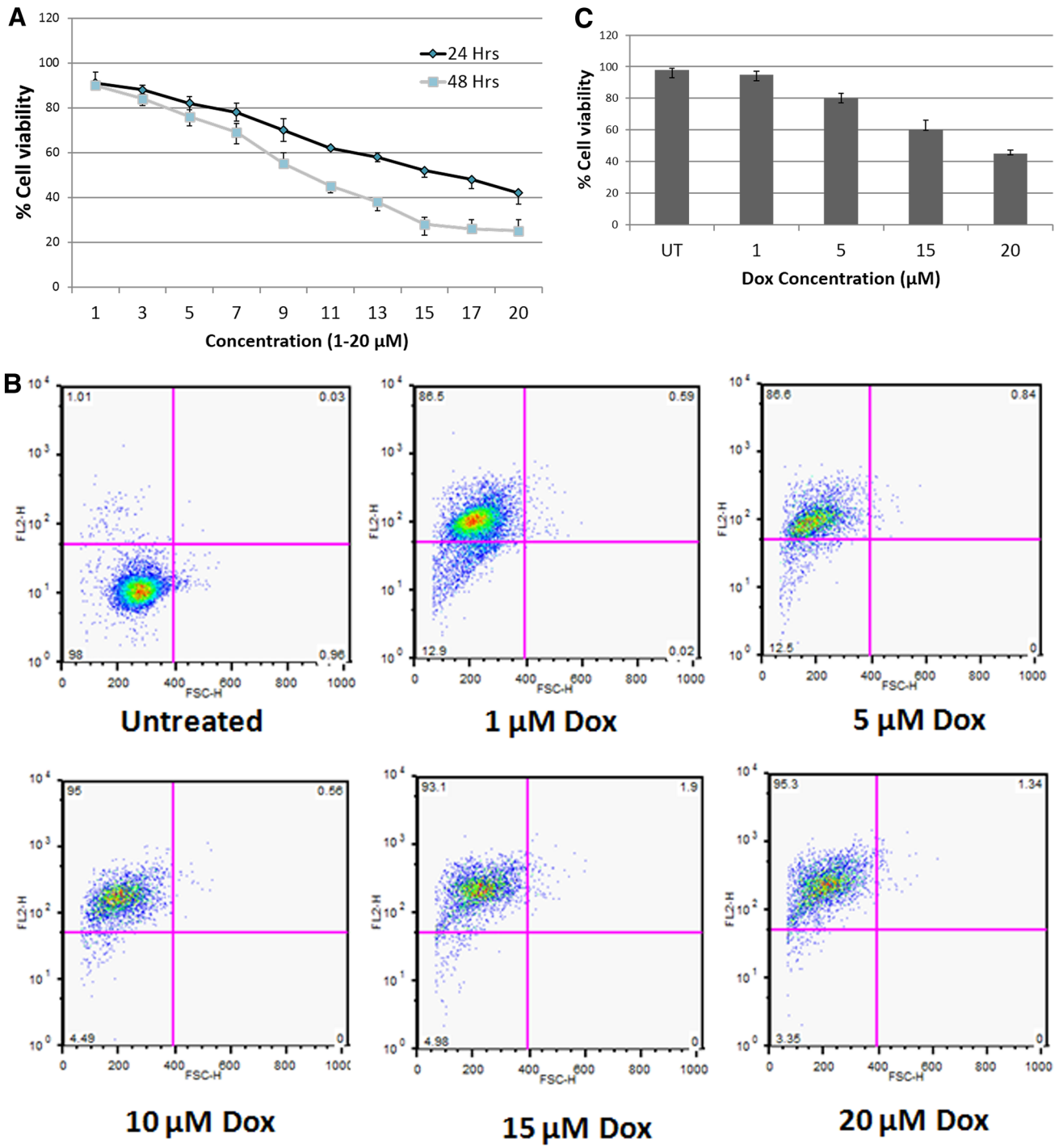

Fig. 1 Concentration-mediated deleterious effect of Dox. **a** MTT assay for Dox ranging from 1 to 20 µM for 24 and 48 h. Cell death was significant at the higher concentrations of Dox. **b** Dox concentration-mediated uptake in H9C2 cells by FACSCalibur analysis. **c** Trypan blue staining to study the cell death and proliferation in response to different Dox concentrations (*$p < 0.05$)

inhibition as evident by total concentration of cells present in different experimental groups also suggested Dox-induced deleterious effects on cardiomyoblasts, where pre and parallel curcumin treatments prevented and potentiated these effects, respectively. Total concentration of cells was decreased by two folds in Dox-treated cells as compared to control and it was further decreased by 1.3-fold in parallel treated cells. However, cells pre-treated with curcumin showed increased cell concentration by 0.7-fold as compared to the Dox-treated cells (Fig. 3a). Giemsa staining confirmed the findings obtained in the previous analysis, suggesting Dox induced altered cellular morphology and

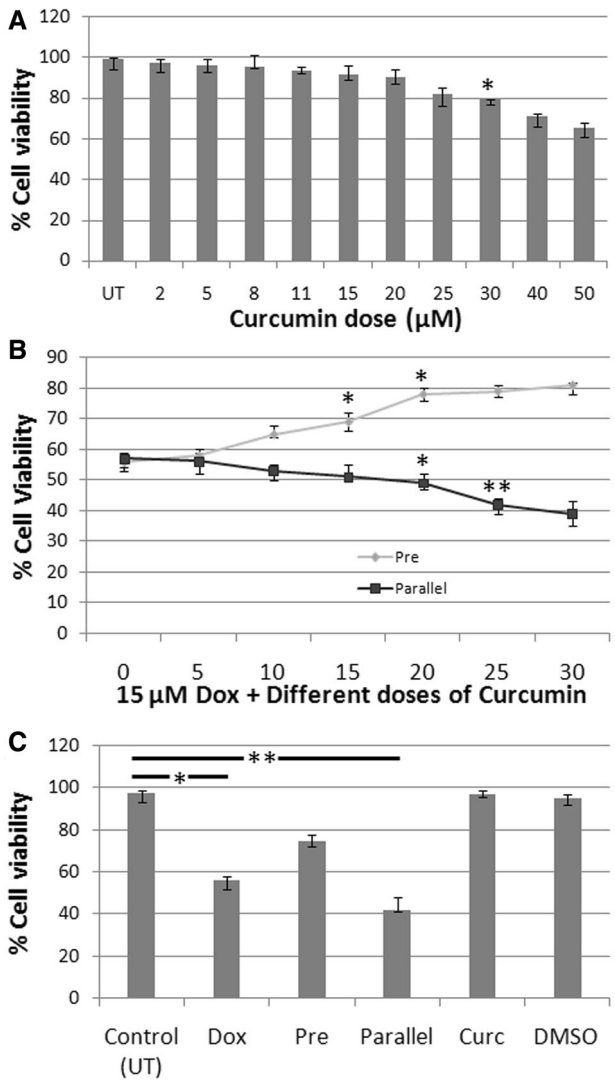

Fig. 2 Effect of different concentrations of curcumin on Dox induction. **a** MTT assay for curcumin where no significant cell death was observed up to the concentration of 30 μM. **b** MTT assay to optimise the concentration of curcumin for pre and parallel treatment on Dox-induced cardiotoxicity. **c** Trypan blue staining to study cell proliferation in presence of Dox and curcumin ($*p < 0.05$)

pre-treatment of curcumin supported the cells to maintain their integrity as evident by the two fold reduction in cellular size in Dox-treated cells (Fig. 3b). Nuclear deformities occur in response to stress and displayed in the form of DNA fragmentation and nuclear shrinkage. These effects were observed by haematoxylin–eosin and fluorescent DAPI nuclear staining. Analysis of nuclear morphological alterations also confirmed that Dox induces variations in cells and curcumin pre-treatment protected and parallel treatment potentiated these nuclear changes (Fig. 3c). Nuclear morphological alterations were also observed in DAPI-stained Dox and curcumin parallel groups, whereas pre-treatment of curcumin maintained nuclear integrity thereby suggesting that mode of curcumin treatment could be crucial for its response in Dox-induced toxicity at cellular and nuclear levels (Fig. 3d).

Pre-treatment of curcumin suppresses Dox-induced ROS production by enhancing the cellular anti-oxidant ability of cells

ROS production in the presence of Dox and anti-oxidant capacity of curcumin were studied by various ROS assays. Increased superoxides production in cell treated with Dox alone and curcumin parallel treatments was witnessed by NBT assay, which was decreased by approximately two fold in pre-treated curcumin group (Fig. 4a, b). DCFH-DA assay displayed increased intracellular ROS production in cells treated with Dox and further exaggerated with parallel curcumin treatment. However, decrease in ROS production up to two fold observed in cells pre-treated with curcumin validated the results that curcumin exerts mode-dependent opposite effects on Dox-induced toxicity (Fig. 4c). Net fluorescence intensity of the eluted stains also represented similar effects (Fig. 4d). We observed that pre-treatment with curcumin reduced the superoxide ions in cells as measured by NBT and DCFH-DA assay. ROS-mediated responses of Dox were further explored by studying the effect on two major anti-oxidant enzymes-SOD and catalase. Inhibitory photochemical reduction of NBT was studied for analysing SOD activity and H_2O_2 reduction was studied for catalase activity. Dox treatment showed ROS mediated modulation of the inbuilt cellular anti-oxidant enzymes. Pre-treatment of curcumin was found to increase activities of both SOD and catalase, whereas significantly reduced anti-oxidant activity was observed in parallel curcumin treatment (Fig. 4e, f).

Pre-treatment of curcumin upholds mitochondrial integrity and caspases

The mitochondrial permeability was studied by Rhodamine 123 staining and it was observed that in the presence of Dox and curcumin parallel treatments, it was decreased by 2- and 2.5-fold, respectively, as compared to control cells as evident by Rhodamine fluorescence. Significant increase in fluorescence in curcumin pre-treated cells suggested the intact mitochondrial membrane (Fig. 5a). Next we observed the caspase activation in response to the Dox and curcumin treatments. Colorimetric analysis of initiator and effector caspases demonstrated elevated levels of the overall caspase activity in cells treated with Dox and curcumin parallel groups. Expression of initiator caspases 2 and 9 in Dox and parallel groups was approximately 2- and 2.5-fold higher as compared to control cells, whereas pre-treatment with curcumin showed expression comparable to

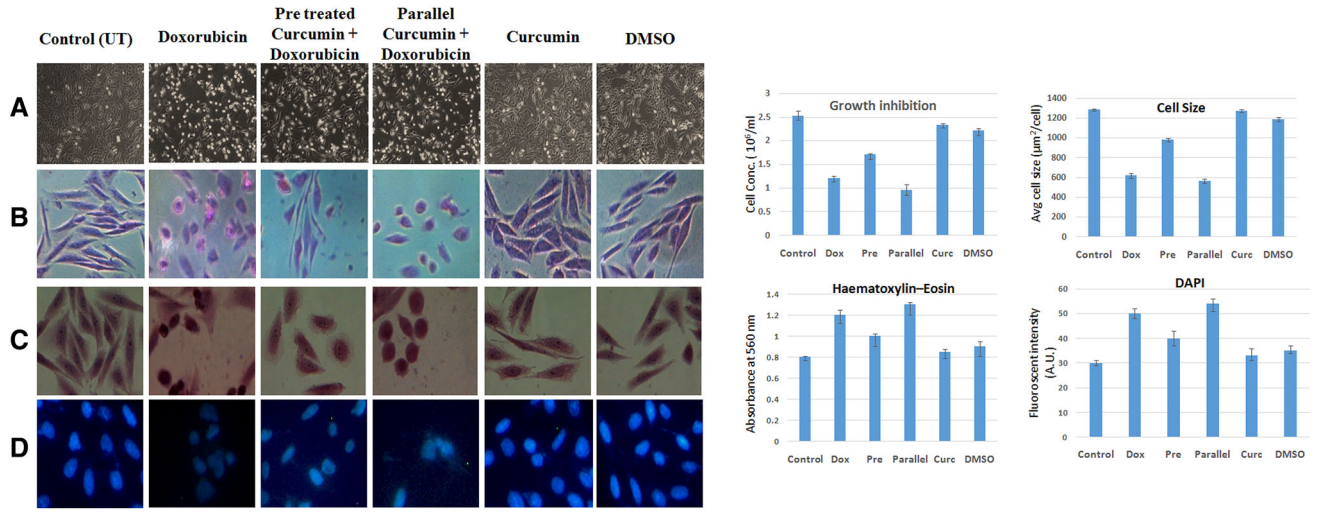

Fig. 3 Cellular and nuclear alterations in cardiac cells morphology upon Dox and curcumin treatment. **a** H9C2 cells in each experimental group were captured under the microscope at ×10 magnification. Significant cell death was observed in the presence of Dox. Total cell concentration was evaluated by Countess® II Automated Cell Counter. **b** Giemsa staining to study the cellular alterations in response to different treatments. The cell size was quantified by NIH ImageJ software. **c** Haematoxylin–Eosin staining to observe the changes in both nuclear and cellular morphology. The eluted stain from the treated cells was quantified. **d** DAPI staining for nuclear alterations was done and the fluorescence intensity was measured by spectrofluorometer. All the images were captured at ×100 magnification ($*p < 0.05$)

the control cells. Expression of effector caspase 3 was 3- and 4-fold higher in Dox and parallel groups, respectively. Although two fold increase in caspase 9 expression in pre-treated group was observed, it was less as compared to Dox and parallel groups (Fig. 5b). This suggested the up-regulation of apoptotic signals in the presence of Dox and parallel treatment and significant downregulation in curcumin pre-treatment in cardiomyoblasts.

Dox exerts growth inhibition and induces apoptotic cellular death, whereas pre-treatment of curcumin prevents this effect

Cell cycle analysis for G1/S and G2/M transitions was studied by FACSCalibur where deconvoluted cellular DNA content was observed by propidium iodide stain and frequency histograms revealed the distribution of cells in three major phases of the cycle (G1/S/G2/M). Also, the apoptotic cells were detected based on the fractional DNA content. The single time-point measurement revealed the percentage of cells in G1/S/G2/M, in the different experimental groups. Dox-treated cells were found to be inhibited in the sub-G1 phase of cell cycle as compared to the control cells where 18.9 and 17.1% cells were present in S and G2/M phase, respectively. The ratio was reduced by six fold in cells with parallel treatment of curcumin suggesting significant growth inhibition. Pre-treatment with curcumin demonstrated the growth distribution pattern similar to the control cells (Fig. 6a, b). It was observed that majority of the cells were inhibited in Sub G-1 when treated with Dox alone or parallelly treated with curcumin and Dox. More number of cells in S-phase in curcumin pre-treated cells suggested that curcumin pre-treatment plays a major role in reversing the Dox-induced growth inhibition. Similar results were obtained for G2/M transition. The cellular death was further characterised by TUNEL assay where significantly more number of TUNEL positive cells were observed in the presence of Dox and curcumin parallel treatments. The number of cells were also reduced by two fold in cells pre-treated with curcumin, which suggested lesser cell death in the presence of curcumin pre-treatment (Fig. 6b).

Expression of apoptotic and oxidative stress markers displays Dox-mediated deleterious effects and curcumin pre-treatment-mediated preventive effects

Expression of anti-apoptotic marker Bcl_2 was found to be increased in cells pre-treated with curcumin and decreased in Dox and parallel treatments which thereby validated our previous observations. These effects of curcumin were also mediated by pro-apoptotic marker Bax as its expression was increased in Dox and curcumin parallel treated groups and found to be decreased in curcumin pre-treated cells (Fig. 7). Hence, this suggested that increased cardiac cellular apoptosis in presence of Dox can be prevented by pre-treatment of curcumin. Expression of oxidative stress markers including anti-oxidant enzymes showed reduced expression in the presence of Dox and curcumin parallel

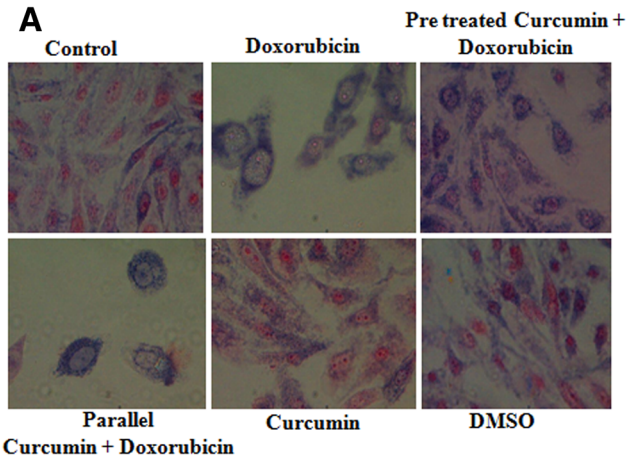

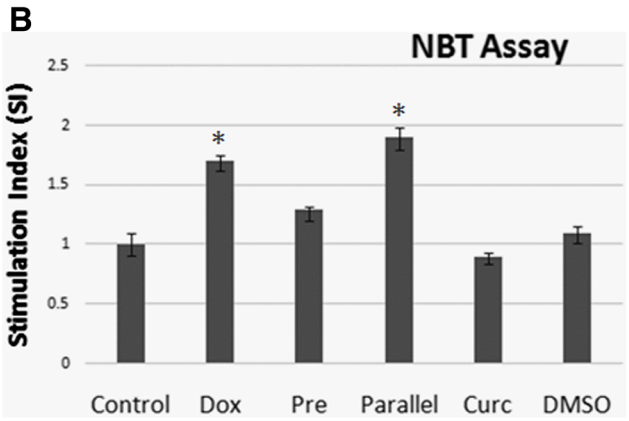

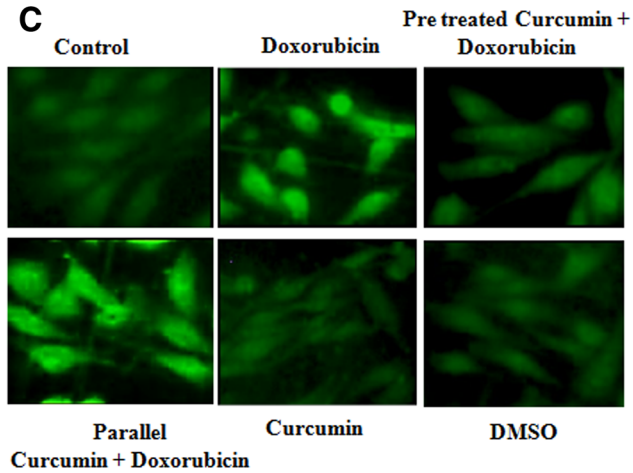

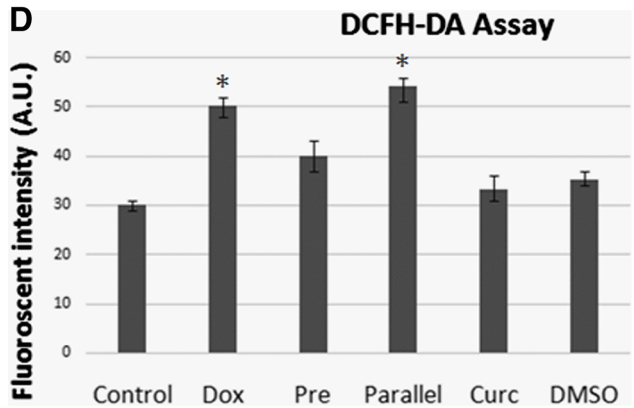

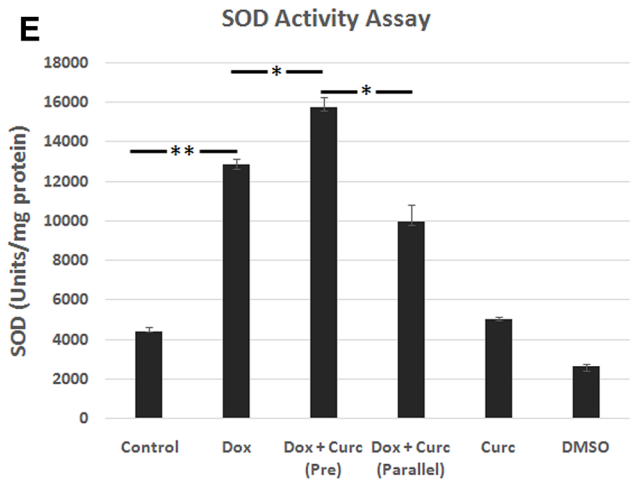

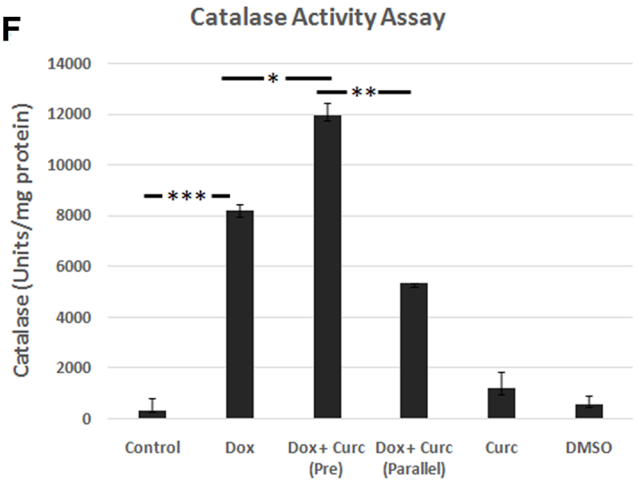

Fig. 4 Effect of Dox and curcumin on ROS production and anti-oxidative enzyme activity in H9C2 cells. **a** Nitroblue tetrazolium (NBT) reduction to formazan blue crystals by cellular superoxide was visualised at ×100 magnification. **b** Spectrophotometric analysis by solubilising the crystals from the cells and quantified at 630 nm. **c** DCFH-DA assay to measure the intracellular ROS production. **d** Net fluorescence of the eluted stain from all the cells was measured by spectrofluorometer and plotted. **e** Superoxide Dismutase (SOD) activity assay. **f** Catalase activity assay. Values indicated as U/mg protein extract for the enzymatic activity (*$p < 0.05$)

treatments, whereas pre-treatment with curcumin demonstrated higher expression thereby resulting in reducing Dox-mediated oxidative stress in cardiomyoblasts.

Discussion

The present study was conducted to explore the effects of curcumin at different modes of treatment (pre and parallel) on Dox-mediated cardiotoxicity. Curcumin being a multi-beneficial compound with both cardioprotective as well as anti-cancerous potential may provide a safer and lesser toxic alternative for the drugs associated with various side effects [49]. At present, cardiotoxicity of anti-cancer therapy is a key safety concern due to the adverse effects on cardiovascular system. It has become a major cause for drug failure and a major apprehension for developing cancer therapeutics and drug discovery. Curcumin and Dox synergism has been investigated with respect to tumour vasculature in anti-angiogenic cancer therapies but no effect on cardiac cell survival has been established for this combination therapy [50]. This study addresses the dual responses of curcumin cited in various literature. We performed time-dependent comparative analysis of curcumin to understand its mode of action in Dox-induced toxicity.

Fig. 6 Cellular death characterisation. **a** Sub-G1 growth analysis to reveal the single time-point measurement of the percentage of cells in G1/S/G2/M phase. **b** Graphical representation of cell cycle analysis of cells treated with Dox and curcumin at different time points. **c** TUNEL assay for detecting apoptotic cells in H9C2 cells induced with Dox and curcumin as shown in fluorescent micrographs. Mean percentage TUNEL positive cells was evaluated in each experimental group ▶

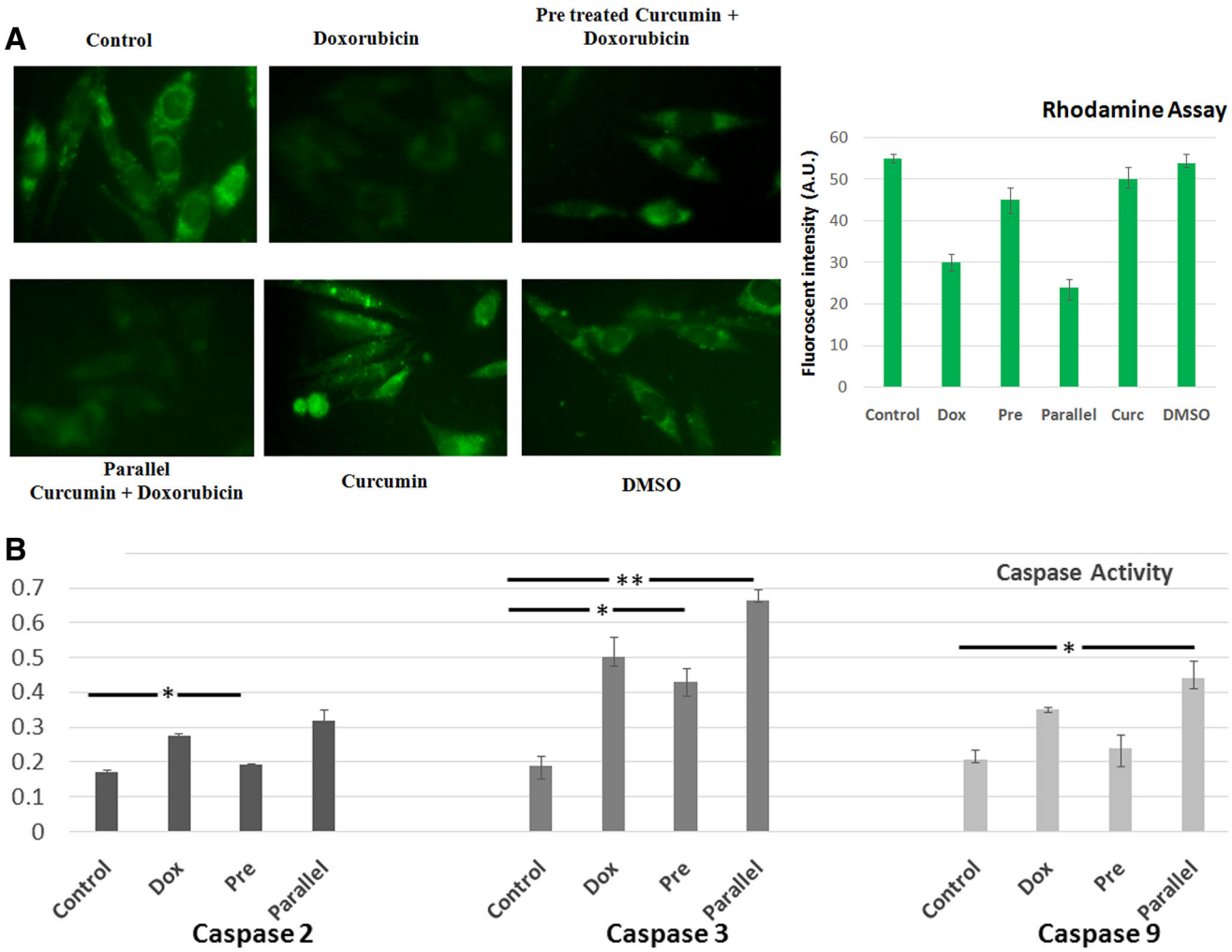

Fig. 5 Effect of Dox and curcumin on mitochondrial membrane integrity and expression of initiator and effector caspases. **a** Rhodamine 123 staining to study the altered mitochondrial membrane potential at ×100 magnification. **b** Caspase activity was evaluated by colorimetric assay by using specific caspase substrate. Pre-treatment of curcumin showed significantly decreased expression of overall caspase activity as compared to Dox and parallel groups (*$p < 0.05$)

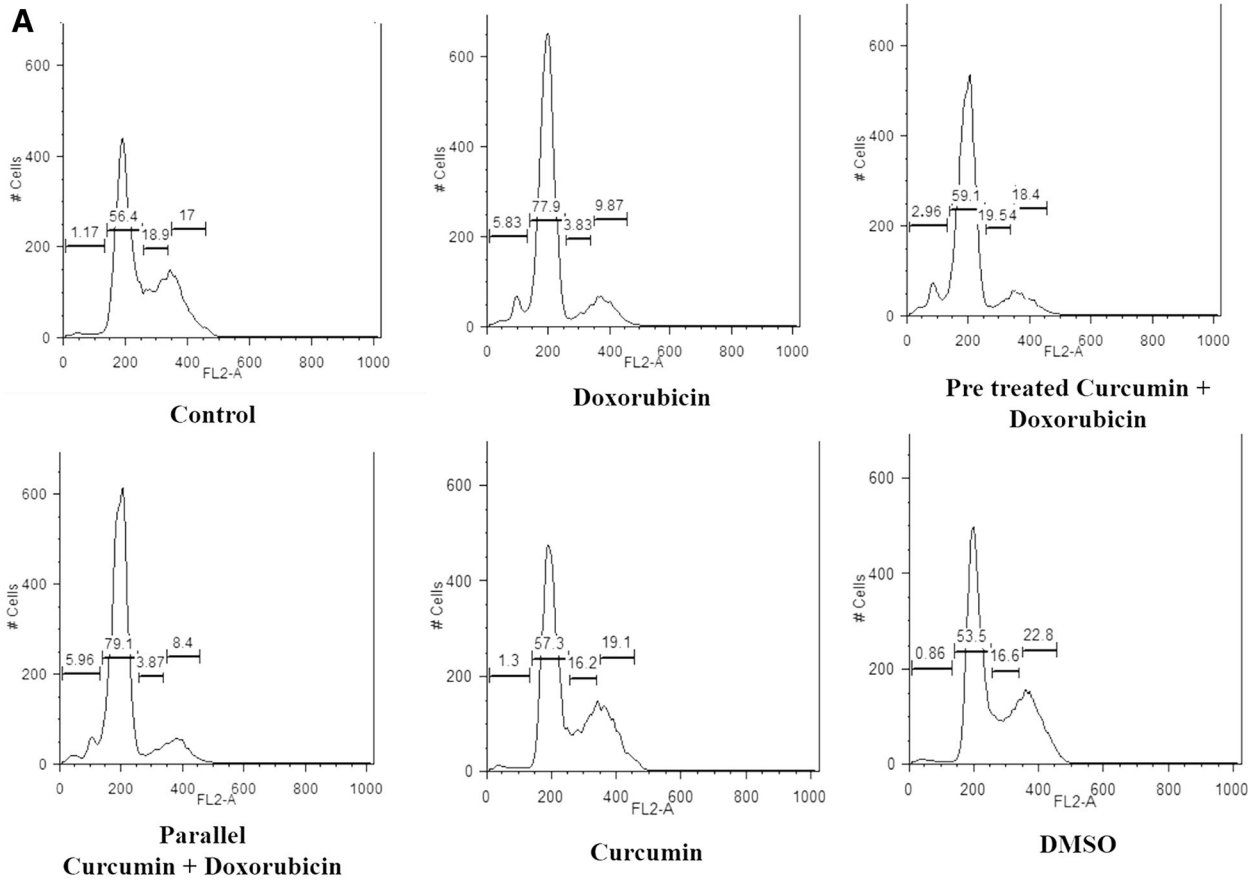
A
Cells
FL2-A
1.17
56.4
18.9
17
Control
5.83
77.9
3.83
9.87
Doxorubicin
2.96
59.1
19.54
18.4
Pre treated Curcumin + Doxorubicin
5.96
79.1
3.87
8.4
Parallel Curcumin + Doxorubicin
1.3
57.3
16.2
19.1
Curcumin
0.86
53.5
16.6
22.8
DMSO

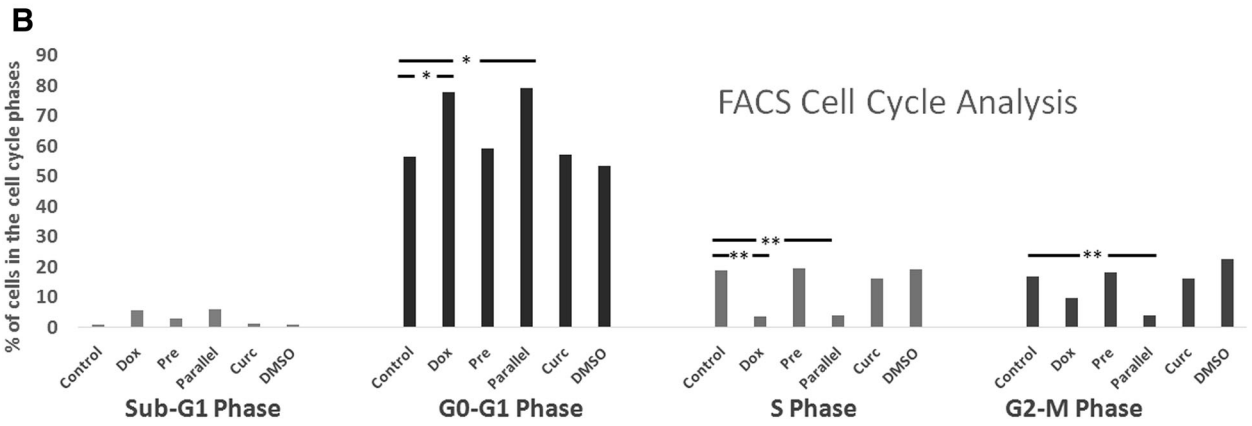
B
FACS Cell Cycle Analysis
% of cells in the cell cycle phases
Control
Dox
Pre
Parallel
Curc
DMSO
Sub-G1 Phase
G0-G1 Phase
S Phase
G2-M Phase

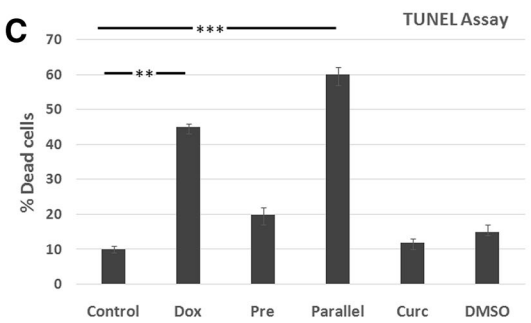
C
TUNEL Assay
% Dead cells
Control
Dox
Pre
Parallel
Curc
DMSO

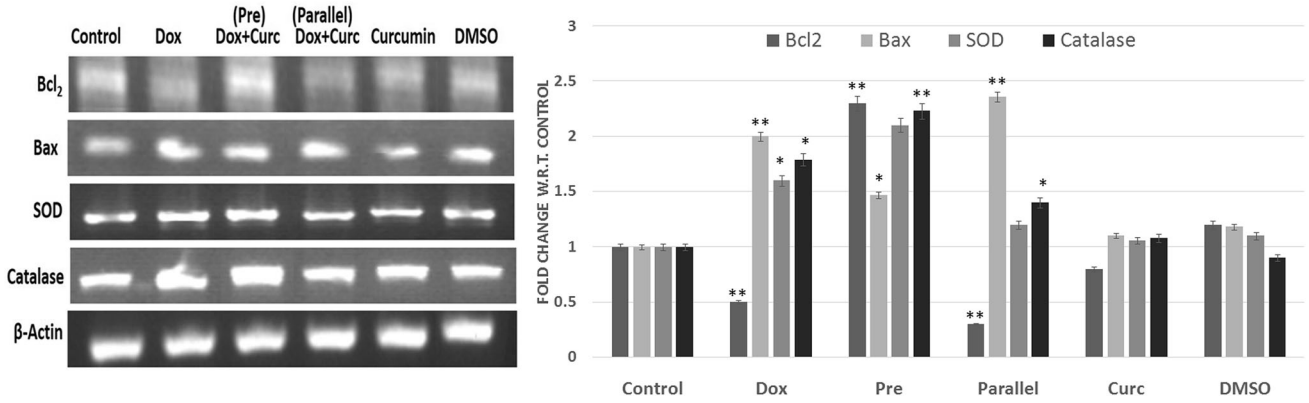

Fig. 7 RT-PCR analysis of SOD, Catalase, pro- and anti-apoptotic genes. Pre-treatment of curcumin suppresses the dox-induced death responses. Fold change with respect to control was calculated after normalisation using ImageJ software and plotted (*$p < 0.05$)

Three different time points of curcumin treatment (pre, parallel and post) were initially screened and we observed extensive cell death in the post treatments of curcumin, possibly due to the prolonged Dox exposure in the cardiomyoblasts. Interestingly, we observed that parallel treatment with curcumin potentiates the Dox-induced toxicity while pre-treatment with curcumin protected cells from the Dox-induced alterations. Therefore, pre and parallel treatments were selected for the subsequent experiments as they showed opposite effects.

Time-dependent cell viability studies confirmed 20 μM curcumin as cardioprotective concentration since it displayed up to 80% cell viability. These concentrations were also confirmed by FACS and trypan blue exclusion assays. The cardioprotective concentration of curcumin used in this study has human physiological relevance; however, alternative modes curcumin administration should be considered to enhance its absorption and bioavailability in vivo [51]. The Dox and curcumin-mediated effects on morphology were then studied, as it is an initial stress marker in cardiac cells. Cardiac myocytes are terminally differentiated cells and respond to stress by altering their size initially, thereby depicting a compromised cellular morphology, but prolonged stress leads to cellular death. The comparison between the cellular and nuclear changes in the six experimental groups confirmed that pre-treatment of curcumin resisted the alterations induced by Dox and parallel treatment with curcumin potentiating the Dox effects. As ROS over production is a key mediator of Dox-induced cardiotoxicity, we next examined the effect of curcumin on intracellular ROS levels by different microscopic and spectrophotometric assays [52]. Curcumin, being an anti-oxidant molecule, known to assists cells undergoing ROS disbalance to amplify the anti-oxidative enzymes' output. Curcumin has shown to regulate the expression of anti-oxidant enzymes and growth factors but its response in Dox-induced cardiotoxicity has not been clearly understood [53]. We concluded that curcumin parallel treatment led to compromised inbuilt anti-oxidant machinery but pre-treatment enhanced the expression of anti-oxidant enzymes thereby resisting the Dox-induced alterations. The imbalance in the inbuilt anti-oxidant enzymes suggested a critical role played by curcumin in maintaining the cellular anti-oxidant activity thereby helping in reducing Dox-induced oxidative stress. The involvement of mitochondria in the stress induced by Dox and curcumin-mediated responses were analysed by mitochondrial membrane permeability. Mitochondria play an important role in maintaining normal cellular functioning and generating stress responses by ROS production and apoptosis [54]. The mitochondrial permeability transition is an important step in the induction of cellular death via apoptosis during which the electrochemical gradient across the mitochondrial membrane collapses. The mitochondrial membrane alterations disturb the basic functioning of mitochondria and hamper the cellular functions. Alterations in mitochondrial integrity in Dox and curcumin-treated cardiomyoblasts established a relationship between altered membrane potentials in the respective treatments. Involvement of caspase activation in response to mitochondrial stress was further studied to analyse the involvement of intrinsic apoptotic pathways in Dox and curcumin-mediated effects. Caspases play an important role in the execution phase of apoptosis and are responsible for various associated biochemical and morphological alterations. The expressions of initiator caspases (Caspase 2 and 9) and effector caspase (Caspase 3) were therefore studied and it was observed that pre-treatment significantly reduced the Dox-induced exaggerated levels of caspases in vitro. This suggested that mitochondria played an important role in Dox and curcumin-mediated events in vitro and resulted in caspase-mediated cellular death in response to Dox and curcumin parallel treatments. Also, supplementing cardiac cells with curcumin prior to Dox

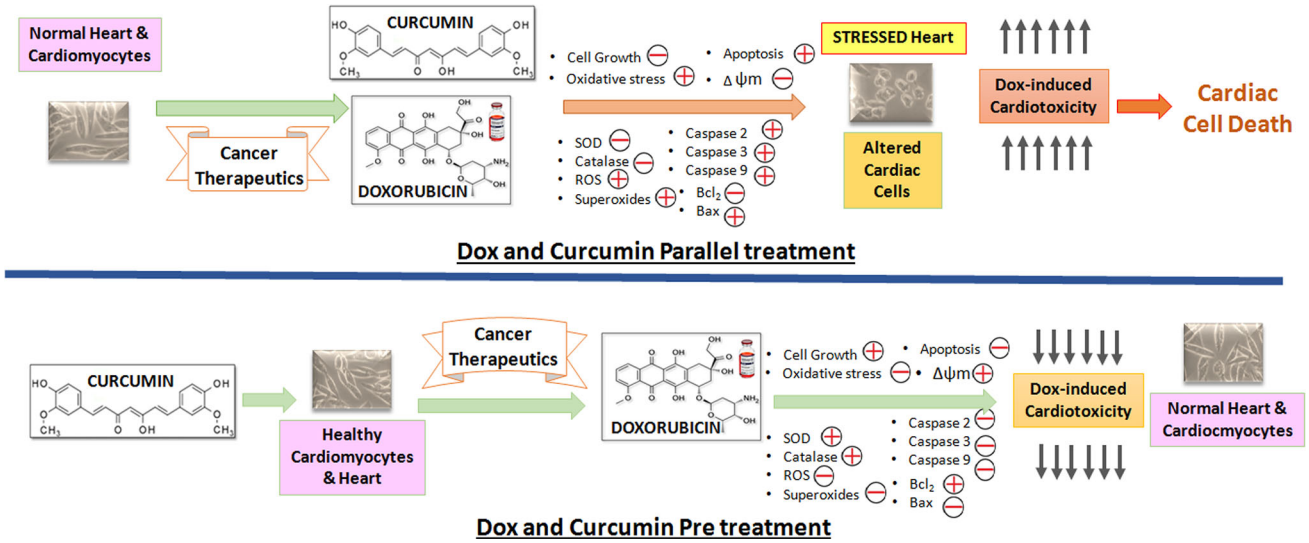

Fig. 8 Working model of the study: Curcumin exerts time-dependent responses on Dox-induced cardiotoxicity where parallel treatment potentiates and pre-treatment suppresses the Dox-induced toxicity in H9C2 cardiomyoblasts

treatment resisted the same. As morphological studies initially revealed that Dox mediates growth inhibition in cardiac cells (Fig. 3a), this was further characterised by cell cycle analysis as G1/S and G2/M phase arrest has been witnessed in Dox-induced cell death [55]. The cellular death and proliferation was further validated by TUNEL assay and the more number of TUNEL positive cells in the presence of Dox confirms the programmed cell death and pre-treatment with curcumin showed reduction in Dox-induced cellular death.

To further explore the molecular mechanisms involved in curcumin-meditated responses in Dox-induced stress, we evaluated the effect of curcumin on the expression of different oxidative and cellular death markers including Bcl_2, Bax, SOD and catalase. Increased levels of anti-apoptotic marker Bcl_2 in curcumin pre-treated group confirmed the cardioprotection. Also, increased expression of pro-apoptotic marker Bax in Dox-treated cardiac cells validated the Dox-induced cardiotoxicity in myoblasts. The cellular collapse is thought to occur through the formation of pores in the mitochondria by dimerized Bax or activated Bid, Bak or Bad proteins [56]. The results indicated that pre-treatment of curcumin exerts its cardioprotective role by modulating mitochondrial-dependent activities including ROS production, caspase activation and apoptosis.

In summary, our data suggested that Dox exhibits cardiotoxicity in vitro and pre-treatment of cells with curcumin is able to suppress the Dox-mediated effects. The overall exaggerated effect of Dox in the parallel treated groups may be justified from the report where it was suggested that anti-oxidants reduced the effect of conventional cytotoxic therapies and might be harmful for the patients [57]. Our findings also answer the cardiotoxicity issues of curcumin raised by Hosseinzadeh et al. in their study where curcumin treatment was given 1 h prior to the Dox treatment which was comparable to the parallel treatment in our study [30]. As per our findings, we infer that the duration of pre-treatment of curcumin is to be taken care of to obtain the significant protection. We propose that when cells are pre-treated with curcumin, cells are prepared to combat the Dox-induced effects. The survival stress boosting threshold of tolerating the toxicity increases and results in resisting the side effects of Dox. However, when cells are treated concomitantly with Dox and curcumin, cells are exposed to the Dox-mediated effects much before curcumin could convey its protective effects, thereby resulting in the toxicity. Pre-treatment with curcumin provides a buffering capacity to the cells by enriching the anti-oxidative pathways as well as the cell survival signals (Fig. 8). The results of the present work may be applicable to native cardiomyocytes and furthermore, the potential preventive activity of curcumin should be evaluated in in vivo systems using well standardised preparations with high bioavailability and improved efficacy for developing cardio-oncological therapeutic interventions.

For future studies, expression analysis at the transcriptome and proteomic level is required to derive the mechanisms of mode-dependent curcumin effects and other signalling pathways. For this, a well-known transcription factor—NF-kB, can be explored in detail as it is responsible for differential gene expression, regulating the expression of cell survival genes—Bcl_2 and Bax; metastasis and cellular proliferation—COX-2 and cyclin D1. Curcumin and Dox have also been shown to modulate the NF-kB expression in the cells via different pathways including PI-3K/Akt. [58–62]. Literature also supports that

inhibition of NF-kB with curcumin attenuates apoptosis and prevents cardiac complications [63]. Therefore, investigating the role of curcumin in Dox-mediated NF-kB overexpression may help in revealing the mode-dependent effects of curcumin. Also, the role of other anti-oxidants should be studied for such mode-dependent effects against drug-induced cardiotoxicity. In this regard, few examples, including silymarin, resveratrol, have been shown cardioprotective properties by targeting drug-induced oxidative stress in the cardiac system [64, 65]. Cecen et al. showed that pre-treatment of silymarin resulted in significant decrease in nitric oxide levels generated by Dox thereby preventing rats from multiple organ toxicity [66]. Lou et al. showed that 24 h pre-treatment of resveratrol in H9C2 cells protects against Dox-induced endoplasmic reticulum stress by activating Sirt1 pathway [67].

Conclusion

Drug-induced cardiotoxicity has become a major complication of cancer chemotherapies and there is a key requirement of identification of safer compounds to assist in the treatment for reduced toxic effects. The present study suggests that pre-treatment of curcumin can be considered in cancer therapeutic applications for reducing the cardiotoxicity. In vivo validation of these findings is required to establish the exact mechanism of mode-mediated curcumin effects. Also, further studies should be conducted to increase the efficacy and bioavailability of curcumin. The outcome of this study can also be useful in reframing the current chemotherapeutic interventions.

Acknowledgements This work was supported by a research grant awarded to Dr. Vibha Rani by the Department of Biotechnology (DBT), Government of India (BT/PR3978/17/766/2011). We acknowledge the Department of Biotechnology, Govt. of India and Jaypee Institute of Information Technology, deemed to be University for providing the funds and infrastructural support. We also acknowledge Dr. Manish Sharma, Scientist D, Peptide and Proteomics Division, Defence Institute of Physiology and Allied Sciences (DIPAS), DRDO, Delhi, India, for providing FACS facility.

Compliance with ethical standards

Conflict of interest There is no conflict of interest among the authors of the manuscript.

References

1. World Health Organization, Media Centre, Fact Sheets (2014) The top 10 causes of death. http://www.who.int/mediacentre/factsheets/fs310/en/. Accessed 28 April 2016
2. Cohen D (2010) Rosiglitazone: what went wrong? Brit Med J 341:c4848
3. Dykens JA, Will Y (2007) The significance of mitochondrial toxicity testing in drug development. Drug Discov Today 12:777–785
4. Gwathmey JK, Tsaioun K, Hajjar RJ (2009) Cardionomics: a new integrative approach for screening cardiotoxicity of drug candidates. Expert Opin Drug Metab Toxicol 5:647–660
5. Sun SX, Lee KY, Bertram CT, Goldstein JL (2007) Withdrawal of COX-2 selective inhibitors rofecoxib and valdecoxib: impact on NSAID and gastroprotective drug prescribing and utilization. Curr Med Res Opin 23:1859–1866
6. Chatterjee K, Zhang J, Honbo N, Karliner JS (2010) Doxorubicin cardiomyopathy. Cardiology 115(2):155–162
7. Volkova M, Russell R (2011) Anthracycline cardiotoxicity: prevalence, pathogenesis and treatment. Curr Cardiol Rev 7:214–220
8. Zordoky BNM, Anwar-Mohamed A, Aboutabl ME, El-Kadi AOS (2010) Acute doxorubicin cardiotoxicity alters cardiac cytochrome P450 expression and arachidonic acid metabolism in rats. Toxicol Appl Pharmacol 242:38–46
9. Sardao VA, Oliveira PJ, Holy J, Oliveira CR, Wallace KB (2009) Morphological alterations induced by doxorubicin on H9c2 myoblasts: nuclear, mitochondrial, and cytoskeletal targets. Cell Biol Toxicol 25(3):227–243
10. Albini A, Pennesi G, Donatelli F, Cammarota R, Flora SD, Noonan DM (2010) Cardiotoxicity of anticancer drugs: the need for cardio-oncology and cardio-oncological prevention. J Natl Cancer Inst 102(1):14–25
11. Parasuraman S (2011) Toxicological screening. J Pharmacol Pharmacother 2:74–79
12. Butler MS (2008) Natural products to drugs: natural product-derived compounds in clinical trials. Nat Prod Rep 25:475–516
13. Nobili S, Lippi D, Witort E, Donnini M, Bausi L, Mini E, Capaccioli S (2009) Natural compounds for cancer treatment and prevention. Pharmacol Res 59:365–378
14. Sheu MT, Jhan HJ, Hsieh CM, Wang CJ, Ho HO (2015) Efficacy of antioxidants as a Complementary and Alternative Medicine (CAM) in combination with the chemotherapeutic agent doxorubicin. Integr Cancer Ther 14(2):184–195
15. Thandavarayan RA, Giridharan VV, Arumugam S, Suzuki K, Ko KM, Krishnamurthy P, Watanabe K, Konishi T (2015) Schisandrin B prevents doxorubicin induced cardiac dysfunction by modulation of DNA damage, oxidative stress and inflammation through inhibition of MAPK/p53 signaling. PLoS ONE 10(3):e0119214
16. Li B, Kim DS, Yadav RK, Kim HR, Chae HJ (2015) Sulforaphane prevents doxorubicin-induced oxidative stress and cell death in rat H9c2 cells. Int J Mol Med 36(1):53–64
17. Goel A, Aggarwal BB (2010) Curcumin, the golden spice from Indian saffron, is a chemosensitizer and radiosensitizer for tumors and chemoprotector and radioprotector for normal organs. Nutr Cancer 62(7):919–930
18. De R, Kundu P, Swarnakar S, Ramamurthy T, Chowdhury A, Nair GB, Mukhopadhyay AK (2009) Antimicrobial activity of curcumin against *Helicobacter pylori* isolates from India and during infections in mice. Antimicrob Agents Chemother 53:1592–1597
19. Menon VP, Sudheer AR (2007) Antioxidant and anti-inflammatory properties of curcumin. Adv Exp Med Biol 595:105–125
20. Sikora E, Scapagnini G, Barbagallo M (2010) Curcumin, inflammation, ageing and age-related diseases. Immun Ageing 7:1
21. Srivastava G, Mehta JL (2009) Currying the heart: curcumin and cardioprotection. Cardiovasc Pharmacol Ther 14(1):22–27
22. Pillai GR, Srivastava AS, Hassanein TI, Chauhan DP, Carrier E (2004) Induction of apoptosis in human lung cancer cells by curcumin. Cancer Lett 208:163–170

23. Ahuja S, Kohli S, Krishnan S, Dogra D, Rani V (2011) Curcumin: a potential therapeutic polyphenol, prevents noradrenaline-induced hypertrophy in rat cardiac myocytes. J Pharm Pharmacol 63:1604–1612
24. Chhabra A, Jaiswal A, Malhotra U, Rani V (2011) Effect of curcumin on matrix metalloproteinases screened in norepinephrine induced cardiac hypertrophy. J Comput Int Bioinf 4:1–10
25. Jain A, Atale N, Kohli S, Bhattacharya S, Sharma M, Rani V (2015) An assessment of norepinephrine mediated hypertrophy to apoptosis transition in cardiac cells: a signal for cell death. Chem Biol Interact 225:54–62
26. Kohli S, Chhabra A, Jaiswal A, Rustagi Y, Sharma M, Rani V (2013) Curcumin suppresses gelatinase B mediated norepinephrine induced stress in H9c2 cardiomyocytes. PLoS ONE 8:1–12
27. Manghani C, Gupta A, Tripathi V, Rani V (2016) Cardioprotective potential of curcumin against norepinephrine-induced cell death: a microscopic study. J Microsc 265(2):232–244
28. Carvalho FS, Burgeiro A, Garcia R, Moreno AJ, Carvalho RA, Oliveira PJ (2014) Doxorubicin-induced cardiotoxicity: from bioenergetic failure and cell death to cardiomyopathy. Med Res Rev 34(1):106–135
29. Mitry MA, Edwards JG (2016) Doxorubicin induced heart failure: phenotype and molecular mechanisms. Int J Cardiol Heart Vasc 10:17–24
30. Hosseinzadeh L, Behravan J, Mosaffa F, Bahrami G, Bahrami A, Karimi G (2011) Curcumin potentiates doxorubicin-induced apoptosis in H9c2 cardiac muscle cells through generation of reactive oxygen species. Food Chem Toxicol 49:1102–1109
31. Linnik OO, Drevytska TI, Gonchar OO, Chornyy SA, Kovalyov OM, Mankovska IM (2016) Doxorubicin-induced alterations in pro-and antioxidant balance and their correction by curcumin in the neonatal rat cardiomyocytes culture. FiziolZh 61(5):90–98
32. Imbaby S, Ewais M, Essawy S, Farag N (2014) Cardioprotective effects of curcumin and nebivolol against doxorubicin-induced cardiac toxicity in rats. Hum Exp Toxicol 33(8):800–813
33. Sadzuka Y, Nagamineb M, Toyookac T, Ibukic Y, Sonobe T (2012) Beneficial effects of curcumin on antitumor activity and adverse reactions of doxorubicin. Int J Pharm 432:42–49
34. Swamy AV, Gulliaya S, Thippeswamy A, Koti BC, Manjula DV (2012) Cardioprotective effect of curcumin against doxorubicin-induced myocardial toxicity in albino rats. Indian J Pharmacol 44:73–77
35. Mohamad RH, El-Bastawesy AM, Zekry ZK, Al-Mehdar HA, Al-Said MG, Aly SS, Sharawy SM, El-Merzabani MM (2009) The role of Curcuma longa against doxorubicin (adriamycin)-induced toxicity in rats. J Med Food 12(2):394–402
36. Watkins S, Borthwick G, Arthur H (2011) The H9C2 cell line and primary neonatal cardiomyocyte cells show similar hypertrophic responses in vitro. In Vitro Cell Dev B 47:125–131
37. Zordoky BN, El-Kadi AO (2007) H9C2 cell line is a valuable in vitro model to study the drug metabolizing enzymes in the heart. J Pharmacol Toxicol Methods 56:317–322
38. Plumb JA, Milroy R, Kaye SB (1989) Effects of the pH dependence of 3-(4,5-dimethylthiazol-2-yl)-2,5-diphenyl-tetrazolium bromide-formazan absorption on chemosensitivity determined by a novel tetrazolium-based assay. Cancer Res 49:4435–4440
39. Cummings BS, Schnellmann RG (2012) Measurement of cell death in mammalian cells. Curr Protoc Pharmacol. doi:10.1002/0471141755.ph1208s25
40. Barcia JJ (2007) The giemsa stain: its history and applications. Int J Surg Pathol 15:292–296
41. Kuroiwa T, Xi G, Hua Y, Nagaraja TN, Fenstermacher JD, Keep RF (2009) Development of a rat model of photothrombotic ischemia and infarction within the caudoputamen. Stroke 40:248–253
42. Kapuscinski J, Skoczylas B (1978) Fluorescent complexes of DNA with DAPI (40,6-diamidine-2-phenyl indole dihydro chloride) or DCI (40,6-dicarboxyamide-2-phenyl indole). Nucleic Acids Res 5:3775–3799
43. Manosroi A, Saraphanchotiwitthaya A, Manosroi J (2006) Effects of Pouteria cambodiana extracts on in vitro immunomodulatory activity of mouse immune system. Fitoterapia 77:189–193
44. Wang H, Joseph JA (1999) Quantifying cellular oxidative stress by dichlorofluorescein assay using microplate reader. Free Radical Biol Med 27:612–616
45. Aebi HE (1983) Catalase. In: Bergmeyer HU (ed) Methods of enzymatic analysis, vol 3. Verlag Chemie, Weinheim, pp 273–286
46. Beauchamp C, Fridovich I (1971) Superoxide dismutase: improved assays and an assay applicable to acrylamide gels. Anal Biochem 44:276–287
47. Lincon VJ, Walsh ML, Chen LB (1980) Localization of mitochondria in living cells with rhodamine 123. Proc Natl Acad Sci USA 77:990–994
48. Juan G, Traganos F, Darzynkiewicz Z (2001) Methods to identify mitotic cells by flow cytometry. Methods Cell Biol 63:343–354
49. Pandey KB, Rizvi SI (2009) Plant polyphenols as dietary antioxidants in human health and disease. Oxid Med Cell Longev 2:270–278
50. Barui S, Saha S, Mondal G, Haseena S, Chaudhuri A (2014) Simultaneous delivery of doxorubicin and curcumin encapsulated in liposomes of pegylated RGDK-lipopeptide to tumor vasculature. Biomaterials 35:1643–1656
51. Howells LM, Moiseeva EP, Neal CP, Foreman BE, Andreadi CK, Sun Y, Hudson EA, Manson MM (2007) Predicting the physiological relevance of in vitro cancer preventive activities of phytochemicals. Acta Pharmacol Sin 28(9):1274–1304
52. Octavia Y, Tocchetti CG, Gabrielson KL, Janssens S, Crijns HJ, Moens AL (2012) Doxorubicin-induced cardiomyopathy: from molecular mechanisms to therapeutic strategies. J Mol Cell Cardiol 52:1213–1225
53. El-Bahr SM (2013) Curcumin regulates gene expression of insulin like growth factor, B-cell CLL/lymphoma 2 and antioxidant enzymes in streptozotocin induced diabetic rats. BMC Complement Altern Med 13:368–378
54. Marchi S, Giorgi C, Suski JM, Agnoletto C, Bononi A, Bonora M, Marchi ED, Missiroli S, Patergnani S, Poletti F, Rimessi A, Duszynski J, Wieckowski MR, Pinton P (2012) Mitochondria-ros crosstalk in the control of cell death and aging. J Signal Transduct 329635:1–17
55. Chen HW, Huang HC (1998) Effect of curcumin on cell cycle progression and apoptosis in vascular smooth muscle cells. Br J Pharmacol 124:1029–1040
56. Webster KA (2012) Mitochondrial membrane permeabilization and cell death during myocardial infarction: roles of calcium and reactive oxygen species. Future Cardiol 8(6):863–884
57. D'Andrea (2005) Use of antioxidants during chemotherapy and radiotherapy should be avoided. CA Cancer J Clin 55:319–321
58. Miriyala S, Panchatcharam M, Rengarajulu P (2007) Cardioprotective effects of curcumin. Adv Exp Med Biol 595:359–377
59. Buhrmann C, Mobasheri A, Busch F, Aldinger C, Stahlmann R, Montaseri A, Shakibaei M (2011) Curcumin modulates nuclear factor kappa B (NF-kappaB)-mediated inflammation in human tenocytes in vitro: role of the phosphatidylinositol 3-kinase/Akt pathway. J Biol Chem 286:28556–28566
60. Marquardt JU, Gomez-Quiroz L, Arreguin Camacho LO, Pinna F, Lee YH, Kitade M, Dominguez MP, Castven D, Breuhahn K, Conner EA, Galle PR, Andersen JB, Factor VM, Thorgeirsson SS (2015) Curcumin effectively inhibits oncogenic NF-κB signaling

and restrains stemness features in liver cancer. J Hepatol S0168–8278:301–303
61. Ho WC, Dickson KM, Barker PA (2005) Nuclear factor-kappaB induced by doxorubicin is deficient in phosphorylation and acetylation and represses nuclear factor-kappa B-dependent transcription in cancer cells. Cancer Res 65:4273–4281
62. Wang S, Kotamraju S, Konorev E, Kalivendi S, Joseph J, Kalyanaraman B (2012) Activation of nuclear factor-kappa B during doxorubicin-induced apoptosis in endothelial cells and myocytes is pro-apoptotic: the role of hydrogen peroxide. Biochem J 367:729–740
63. Yeh CH, Chen TP, Wu YC, Lin YM, Lin PJ (2005) Inhibition of NFB activation with curcumin attenuates plasma inflammatory cytokines surge and cardiomyocytic apoptosis following cardiac ischemia/reperfusion. J Surg Res 125:109–116
64. Razavi BM, Karimi G (2016) Protective effect of silymarin against chemical-induced cardiotoxicity. Iran J Basic Med Sci 19(9):916–923
65. Gu J, Hu W, Zhang DD (2015) Resveratrol, a polyphenol phytoalexin, protects against doxorubicin-induced cardiotoxicity. J Cell Mol Med 19(10):2324–2328
66. Cecen E, Dost T, Culhaci N, Karul A, Ergur B, Birincioglu M (2011) Protective effects of silymarin against doxorubicin-induced toxicity. Asian Pac J Cancer Prev 12(10):2697–2704
67. Lou Y, Wang Z, Xu Y, Zhou P, Cao J, Li Y, Chen Y, Sun J, Fu L (2015) Resveratrol prevents doxorubicin-induced cardiotoxicity in H9c2 cells through the inhibition of endoplasmic reticulum stress and the activation of the Sirt1 pathway. Int J Mol Med 36(3):873–880